Available online at www.sciencedirect.com
SCIENCE DIRECT®
Journal of the European Ceramic Society 25 (2005) 233–241
www.elsevier.com/locate/jeurceramsoc

Methylene-bridged carbosilanes and polycarbosilanes as precursors to silicon carbide—from ceramic composites to SiC nanomaterials

Qing-Min Cheng[a,1], Leonard V. Interrante[a,*], Michael Lienhard[b], Qionghua Shen[c], Zhizhong Wu[a]

[a] *Chemistry Department, Rensselaer Polytechnic Institute, Troy, NY 12180-3590, USA*
[b] *NASA Glenn Research Center, MS 77-1, Cleveland, OH 44135, USA*
[c] *Starfire Systems Inc., Saratoga Technology and Energy Park, 10 Hermes Road, Malta, NY 12020, USA*

Available online 11 September 2004

Abstract

Polymeric and oligomeric carbosilanes having Si atoms linked by methylene (–CH_2–) groups were used to prepare nano-sized tubules and bamboo-like SiC structures by both CVD and liquid precursor infiltration and pyrolysis inside of nanoporous alumina filter disks, followed by dissolution of the alumina template in $HF_{(aq)}$. These initially amorphous SiC structures were characterized by SEM, EMPA, TEM, and XRD. Typical outer diameters of the SiC nanotubes (NTs) were 200–300 nm with 20–40 nm wall thicknesses and lengths up to the thickness of the original alumina templates, ca. 60 μm. In the case of the CVD-derived SiC NTs, annealing these structures up to 1600 °C in an Ar atmosphere yielded a nanocrystalline β-SiC or β-SiC/C composite in the shape of the original NTs, while in the case of the liquid precursor-derived nanostructures, conversion to a collection of single crystal SiC nanofibers and other small particles was observed.

Keywords: Organosilicon chemistry; Polycarbosilane; Oligomeric components

1. Introduction

1.1. Background on the precursors employed

Our research in organosilicon chemistry over the past 18 years has centered on the synthesis, study, and application in materials chemistry, of a broad class of carbosilane oligomers and polymers that contain bridging Si–CH_2–Si groups. In addition to single-source CVD precursors to silicon carbide,[1] this research has led to the development of a commercial hyperbranched polycarbosilane precursor to SiC (AHPCS)[2–4] as well as linear polycarbosilanes of the type, $[SiRR'CH_2]_n$, that have been of fundamental interest as silicon analogs of important organic polymers, such as polyethylene[5] and polyvinylidene fluoride,[6] as well as for use in the study of the pyrolytic conversion of polycarbosilanes to SiC.[7]

The synthesis of the hyperbranched polycarbosilane was originally carried out by coupling of the AB_3-type monomer, $ClMgCH_2SiCl_3$, the Grignard reagent of $ClCH_2SiCl_3$, in ether solution, followed by reduction with $LiAlH_4$.[8] The intermediate chlorocarbosilane, having the nominal composition, "$[SiCl_2CH_2]$", but with a hyperbranched structure of the type, $[Cl_3SiCH_2-]_x[-SiCl_2CH_2-]_y[=SiCl(CH_2-)]_z[\equiv Si(CH_2-)]_l$, could be further modified through reactions involving the Si–Cl groups, leading to various final products having a hyperbranched polycarbosilane "core structure". Thus, replacement of Cl by alkoxy was used to obtain a sol–gel precursor, suitable for spin coating of a "$[Si(O)CH_2]_n$" gel that exhibits low-*k* properties,[9] as well as for preparation of a bulk organic-inorganic "$[Si(O)CH_2]_n$" hybrid material and, after pyrolysis, silicon oxycarbide, having high BET surface areas and a sharp peak in the pore size distribution at ca. 2 nm.[10] Replacement of Cl by allyl (–$CH_2CH{=}CH_2$) groups, by using allylMgCl, yields a "$[SiCl_{2-x}(allyl)_xCH_2]$", derivative with as high as 90% allyl substitution (x = 1.8). This highly allyl-substituted deriva-

* Corresponding author.
E-mail address: interl@rpi.edu (L.V. Interrante).
[1] Currently at: Nanomat Inc., 1061 Main Street, North Huntingdon, PA 15642-7425, USA.

0955-2219/$ – see front matter © 2004 Elsevier Ltd. All rights reserved.
doi:10.1016/j.jeurceramsoc.2004.08.005

tive (APCS) can be used to attach various types of side chains through hydrosilation reactions[3] leading, for example, to APCS-PEO side-chain polymers that, when doped with LiX salts, can serve as ionically conductive, Li^+ electrolyte media.[11] Partial substitution with allyl (on the order of 5–10%) prior to reduction of the remaining Cl groups to H with $LiAlH_4$, yields an allylhydridopolycarbosilane (AHPCS) that exhibits high ceramic yield for conversion to a near stoichiometric, amorphous, SiC on pyrolysis to 1000 °C.[12] This relatively air-stable, liquid, polycarbosilane has been widely used as a precursor for SiC matrixes in SiC/SiC and C/SiC composites through polymer infiltration and pyrolysis and as part of a "molding compound" for the fabrication of particulate-reinforced SiC matrix composites and monoliths.[13,14] We have recently found that mixtures of this AHPCS with polyborazylene (pBz) yield, on pyrolysis and subsequent thermal annealing, two-phase ceramic composites with a "polymer-blend" type microstructure and novel mechanical properties, including low hardness and resistance to crack propagation, suggesting their possible use as matrixes or interphases in high temperature ceramic composites.[15]

We now report the application of these carbosilane and polycarbosilane precursors to the preparation of SiC nanostructures by using a templating method that has been used previously to prepare nanotubes and nanofibers of both organic and inorganic materials.[16–20]

1.2. Prior efforts to prepare 1D SiC nanomaterials

Since the discovery of carbon nanotubes in 1991,[21] considerable effort has been focused on the synthesis and processing of "one-dimensional" nano-scale materials such as nanotubes and nanowires due to their potential for applications in various areas of future technology, from the delivery of medicines and detection of biological molecules to the construction of nanoscale electronic and optoelectronic devices. To date, besides carbon, many materials have been prepared in the form of nanotubes, such as BN and BC_2N,[22,23] MoS_2 and WS_2,[24] various oxides (SiO_2, V_2O_5, Al_2O_3, MoO_3),[25] and other nitrides, carbides, and sulfides.[26] Silicon carbide (SiC) is a high performance semiconductor which can be operated at high temperatures, high power and high frequencies, and in harsh environments.[27] SiC is also an important high temperature structural material, which is used in igniters, heating elements, and in high temperature structural composites for both industrial and aerospace applications.[28] While SiC has been obtained by several groups in the form of nanorods,[29–36] relatively little attention has been devoted to the preparation of SiC nanotubes.[37]

Single-crystal β-SiC nanorods with and without amorphous SiO_2 wrapping layers have been prepared by well established methods, including the reaction of $SiO_{(g)}$ with elemental carbon in various forms (including C nanotubes) or with CO,[29–33] the reduction of silica or silica gel with carbon,[34] the direct reaction of Si and C, usually facilitated by a liquid metal "catalyst",[35] and reaction between $SiCl_4$ and CCl_4 with Na metal as the reductant.[36] In view of the high temperature stability of these SiC nanorods, coupled with their unique optical,[30] mechanical,[31] and field emission properties,[32] similar properties might be expected for SiC nanotubes, which could also serve additional roles by virtue of their tubular form. These include their possible use as "nanoreactors" or "nano-test tubes" [19] for high temperature reactions that cannot be carried out in carbon nanotubes, as well as for molecular separations that might depend on the (potentially modifiable) surface properties of the tube interior, as well as their restricted internal diameter. When coupled with the unique optical and electrical properties expected for nanosized, crystalline, SiC, the opportunity for many other types of applications, such as qualitative, and even quantitative, analysis of trace amounts of certain chemicals or biological molecules, can be envisioned.

However, in the case of hollow SiC nanotubes, there are relatively few reports of their successful preparation, and these contain few details regarding the detailed composition, form, and properties of the resultant nanomaterials. One approach has involved what was called "a shape memory synthesis method", in which carbon microfibers and nanotubes were reacted with SiO vapor at 1200–1250 °C, followed by oxidation in air at 600 °C to remove the excess carbon.[38] The product of this reaction was identified as polycrystalline β-SiC by XRD; however, particularly in the case of the products obtained from the CNT conversion, the SiC structures were poorly formed and highly fragmented, with irregular shapes and sizes that only crudely resembled the original multiwall, large diameter (ca. 10 micrometers), carbon nanotubes that were used to prepare them. Nonetheless, these materials had high surface areas and were found to yield promising results when used as a catalyst support material for the selective conversion of H_2S into elemental sulfur.[39] A similar $SiO_{(g)} + 2C_{(s)} \rightarrow SiC_{(s)} + CO_{(g)}$ reaction was employed by Sun et al.[40] on smaller (10–50 nm) diameter MWCNTs to obtain a mixture of products that included mainly SiC nanowires, but which also contained some materials that were described as multiwall SiC nanotubes, based on HRTEM and EELS studies. Finally, Sneddon and co-workers have reported the use of organoborane and polycarbosilane (AHPCS) precursors to obtain boron carbide, boron nitride and silicon carbide nanofibers and nanotubules by pyrolysis in nanoporous alumina templates; however, few details were given in this brief report about the nature of the SiC nanotubes so obtained.[41]

1.3. The template approach to nanorod and nanotube formation

An approach that is finding increasing interest as a source of both nanorods and nanotubes of various materials, including polymers, carbon, metals, semiconductors, and ceramics,[18–20,42] involves the absorption of precursor materials into channels of nanoporous template materials containing monodisperse, cylindrical pores. Both gas phase (CVD)

and solution deposition methods have been employed in this context, with the conversion of precursors to final solid state materials accomplished by electrochemical, thermolytic or chemical reactions. The most commonly used template of this type is made of alumina and derived by anodic oxidization of thin aluminum films.[43] These thin, nanoporous, alumina membranes have become commercially available and are used predominantly for separation and nanofiltration applications.

2. Experimental

2.1. General

Poly(silaethylene) (PSE) was prepared, as previously described,[5(b)] by platinum catalyzed ring-opening polymerization of tetraethoxydisilacyclobutane, followed by $LiAlH_4$ reduction. The particular sample used in this work had a M_n of ca. 3000. A mixture of volatile carbosilanes having the common compositional formula of $[SiH_2CH_2]$, was obtained from Starfire Systems, Incorporated (Malta, NY; SP-4000). A GC/MS analysis of this clear liquid revealed mostly cyclic trisilacyclohexane $[SiH_2CH_2]_3$ (ca. 70%) along with other oligomeric components, such as $[SiH_2CH_2]_n$ (n = 4–8) and/or related isomeric compounds, such as SiH_3CH_2-*cyclo*-$\{-SiHCH_2(SiH_2CH_2)_x-\}$, $x = 2$. A second sample was obtained from Starfire Systems that had approximately the same nominal SiH_2CH_2 composition, but consisted of higher molecular weight oligomers and polymers (M_n = 500–2000).

2.2. Preparation of SiC nanotubes by CVD using a volatile carbosilane mixture

Commercially obtained nanoporous alumina membranes (Whatman Anodisc Membrane Filters) with a thickness of 60 μm and a nominal pore size of around 250 (±50 nm) were used as templates without prior treatment. The CVD template synthesis was carried out in a two-stage tube furnace system. Five grams of the carbosilane precursor held in an alumina boat was placed in the upstream end of a quartz tube and centered in the first tube furnace. A piece of template membrane (ca. 10 cm^2) was placed horizontally in the center of the second (downstream) furnace. Nitrogen (99.9%, 200 sccm) was used as the carrier gas. After flushing the system with nitrogen for ca. 15 min, the second furnace was heated (15 °C/min) to 1000 °C and then the temperature of the first furnace was slowly increased from room temperature to 100 °C (ca. 30 min). The second furnace was maintained at 1000 °C for 1 h after exhaustion of the precursor. During the heating, a black thin film was observed in the quartz tube in the hot zone (1000 °C), corresponding to the deposition of a SiC thin film. Next, the samples were cooled overnight under a constant flow of N_2 and the alumina templates were dissolved by immersing the samples in 49% hydrofluoric acid for 48 h. The resulting black materials (typically 5–10 mg, 0.1–0.2%, based on the amount of precursor used) were then washed thoroughly with deionized water, methanol, and acetone and dried at room temperature.

2.3. Preparation of SiC nanomaterials by heating alumina membranes infused with liquid carbosilanes

Pieces (13 mm diameter) of the alumina membranes were immersed in either pentane solutions of liquid carbosilanes or PSE, and also in the neat liquid precursors, at room temperature in a N_2 filled glove box. After allowing the membranes to stand in contact with the precursors for about 5 min, excess liquids were blotted from one side of the membranes, which were then transferred to an alumina boat and then pyrolyzed in a tube furnace under a flow of high purity N_2 to 1000 °C at 5 °C/min, and held at the final temperature for 2 h. The samples were cooled overnight under a continued flow of N_2. The alumina templates were dissolved by soaking the samples in 49% hydrofluoric acid for 48h. The resulting products were then washed thoroughly with deionized water, methanol, and acetone and dried.

Further heating to 1600 °C was carried out on selected samples of the products obtained from both procedures in an alumina tube furnace. The samples were placed in molybdenum boats and were wrapped with carbon cloth, the ends folded over to cover completely, and tied up with carbon thread, to limit their contact with residual $O_{2(g)}$ in the ambient atmosphere during the annealing experiment. The boats were inserted into the cool end of the alumina furnace tube, which was outside the furnace and, after sealing the tube, were allowed to flush with argon for about 30 min before sliding them (under a counter-flow of argon) into the hot zone which was idling at 800 °C. The furnace temperature was increased at 3 °C/min to 1600 °C, and held at that temperature for 4h. A flowing argon atmosphere was maintained throughout the entire process.

2.4. Analysis of the products

Characterization of the products before and after annealing was carried out by using transmission electron microscopy (TEM: Philips CM-12, 3.14A resolution), high resolution transmission electron microscopy (HRTEM; JEOL JSM-2010 FASTEM, 2.0A resolution, GIF/EELS/EDS), and energy dispersive X-ray spectroscopy (attached to the Philips CM-12 TEM). The SiC tubular materials were also characterized and studied by scanning electron microscopy (SEM: JEOL, JSM-4335FE, 15A resolution, SE + BSE imaging, EDS), X-ray Powder Diffraction (XRD, Cu Kα), and Micro-Raman spectroscopy (Renishaw, AR + Diode lasers). Auger electron spectroscopy (AES), and infrared spectroscopy were also used to verify the presence of crystalline SiC in the annealed samples. TEM samples were prepared by dispersing the powder in alcohol by ultra sonication, dropping onto a holey carbon-coated copper grid, and drying in air. Elemental analyses of the epoxy-mounted samples were carried out by

using a focused beam on a JEOL 733 electron microprobe automated with dQant software from Geller MicroAnalytical, at a current of 25 nA and an accelerating voltage of 15 kV, using the Heinrich ZAF correction model.[44] Standards included BN, SiC, and Al_2O_3, which were calibrated under the same operating conditions. Samples and standards were simultaneously coated with a thin film (roughly 300 Å) of Cr metal to eliminate charging from the electron beam. Analyses were performed by analyzing the K alpha X-ray lines using a LDE1 crystal for C and O, and a TAP crystal for Si.

3. Results and discussion

3.1. CVD-derived SiC nanotubes

Fig. 1 shows typical scanning electron microscopy (SEM) images of a sample of nanotubes prepared by heating up to 1000 °C in a CVD reactor, using a volatile carbosilane mixture as the precursor, after dissolution of the alumina template by using $HF_{(aq)}$. It can be seen that the tubules appear to be uniform, smooth, open on both ends, and straight, with a ca. 250–300 nm outer diameter.

The length of most of these SiC nanotubes is about 60 μm, which is equal to the thickness of the original alumina membrane. We also found that some of the tubules have a branched structure and some have Y junctions, replicating the corresponding features in the original alumina templates. In addition to tube formation, a thin layer of SiC formed on the surface of the templates. The layer serves to hold the tubules in their parallel arrangement after removal of the alumina template, giving a highly aligned configuration (Fig. 2). Ultrasonication in alcohol at room temperature for a short time (ca. 1 min.) is sufficient to break up the SiC thin film and separate the individual nanotubes.

Fig. 3 shows a TEM image of the as-prepared (at 1000 °C) tubules after sonication. It can be seen that the tubules are straight and fairly uniform and have a wall thickness about 20–40 nm, with some gradation in thickness from the ends to the center, where the tubes are the thinnest.

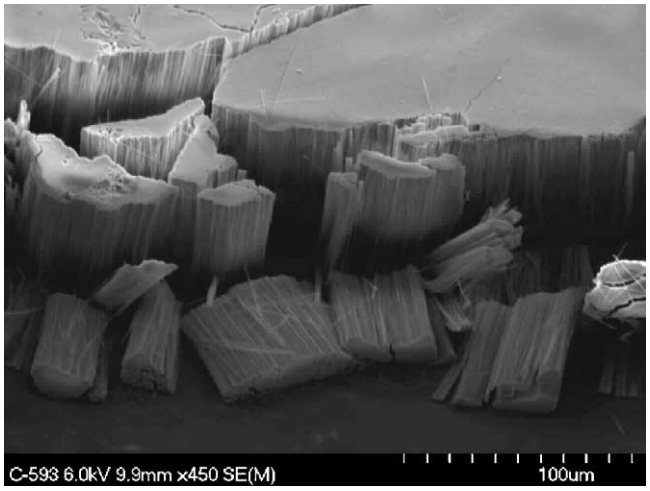

Fig. 2. An assemblage of SiC nanotubes held together by the SiC film formed on the alumina membrane surface, after dissolution of the alumina in $HF_{(aq)}$.

Efforts to make the tube walls thicker by lengthening the deposition time with the precursor carbosilanes failed. In these cases, as the film formed at the surface of the alumina templates became thicker, it tended to close off the opening to the pores, preventing further influx of the precursor. The SAED pattern obtained for these nanotubes (not shown) indicated an amorphous structure for the SiC. The elemental composition of a collection of these as-obtained nanotubes was determined by scanning electron microprobe analysis. Average wt.% values measured for several (9) individual "bundles" of these nanotubes indicated 59.7% Si, 36.0% C, and 3.6% O ($Si_1C_{1.4}O_{0.1}$). Thus, the composition of these nanotubes appears to be that of a C-rich SiC, with ca. 6 mol% oxygen present, probably mainly on the outer and inner wall surfaces of these high surface area samples (estimated at ca. 80 m^2/g).

By virtue of their unique surface chemistry, both the original SiC nanotubes and the silica nanotubes obtained from them by oxidation[45] are of potential interest for nanoscale molecular separations, and as channels or active compo-

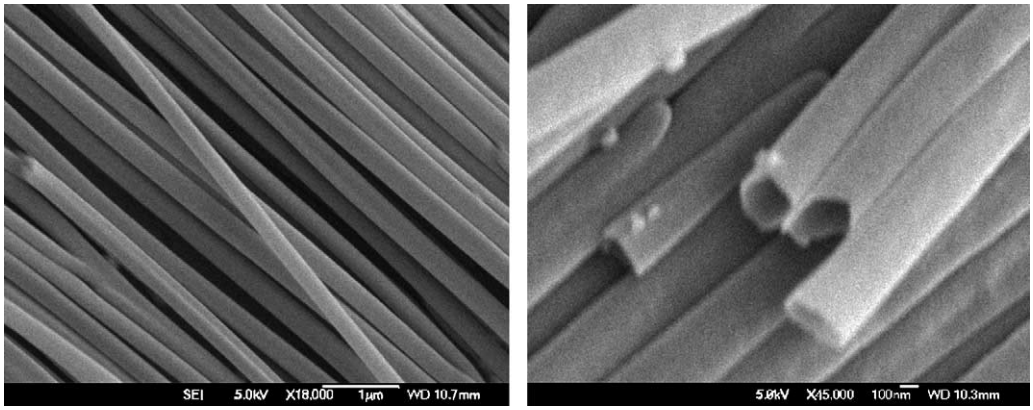

Fig. 1. SEM image of a collection of individual SiC nanotubes, prepared by CVD inside of nanoporous alumina membranes.

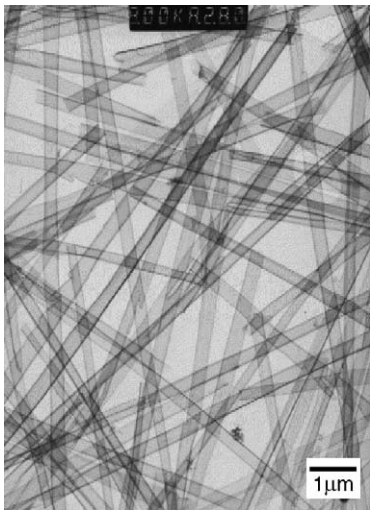

Fig. 3. TEM image for the as-produced, CVD-derived, SiC nanotubes.

nents in microfluidic devices. Thus, unlike carbon nanotubes, which typically undergo significant degradation in order to generate surface functionality sufficient for covalent attachment of organic groups at the tube wall, the Si–OH containing surface of these SiC or SiO_2 nanotubes are well suited to convenient functionalization by using the same type of silylating groups (such as $(MeO)_3Si–R$) that are commonly used for modification of glass surfaces.[46] This should allow dispersal into polymers and organic solvents and changes in hydrophobicity/hydrophilicity, as well as the attachment of groups that are selective for the adsorption of certain chemical and biological species.[47] The optical transparency of silica in particular offers the potential for immobilization of minute amounts of selected, tagged, analytes in a specific region of a functionalized nanotubule where it can be observed by optical absorption or emission methods.

3.2. Results of annealing experiments on the CVD-derived SiC_x nanotubes

Annealing the initially formed, CVD-derived, SiC_x nanotubes at 1600 °C leads to two main kinds of morphology for the resultant partially crystallized products. One type, as shown in Fig. 4a, consisted of tubules having a rough surface and small particles on the tube surface. These tubules had a high degree of crystallization, as indicated by the SAED pattern.

The rings observed in the SAED pattern corresponded to the {1 1 1}, {2 2 0}, {3 1 1} crystal planes of cubic β-SiC. Under high magnification in the TEM, individual SiC particles on the tube surface could be observed. The second type of morphology consisted of nanotubes having smooth surfaces and a relatively low degree of crystallization as nanocrystalline β-SiC (Fig. 4b). The proportion of these two types of nanotubes varied with the batch obtained and, based on separate studies to be reported elsewhere[45] that were carried out by using disilacyclobutane $[SiH_2CH_2]_2$ as a single-source CVD precursor, appears to depend, at least in part, on the purity and composition of the precursor source employed. Thus, the single-source precursor yielded stoichiometric SiC nanotubes that formed an agglomeration of highly crystallized particles upon high temperature annealing. It is well known that even a small amount of excess carbon is effective in limiting the size of the SiC crystallites formed on pyrolysis of organosilicon precursors and its apparent presence in these CVD-derived samples in varying amounts could certainly account for the differences observed in the degree of crystallinity and average SiC grain size in the obtained nanotubes. In addition to possible variations in the precursor composition from batch to batch, it is also possible that changes in the rate of deposition caused by slight variations in the deposition procedure may have contributed

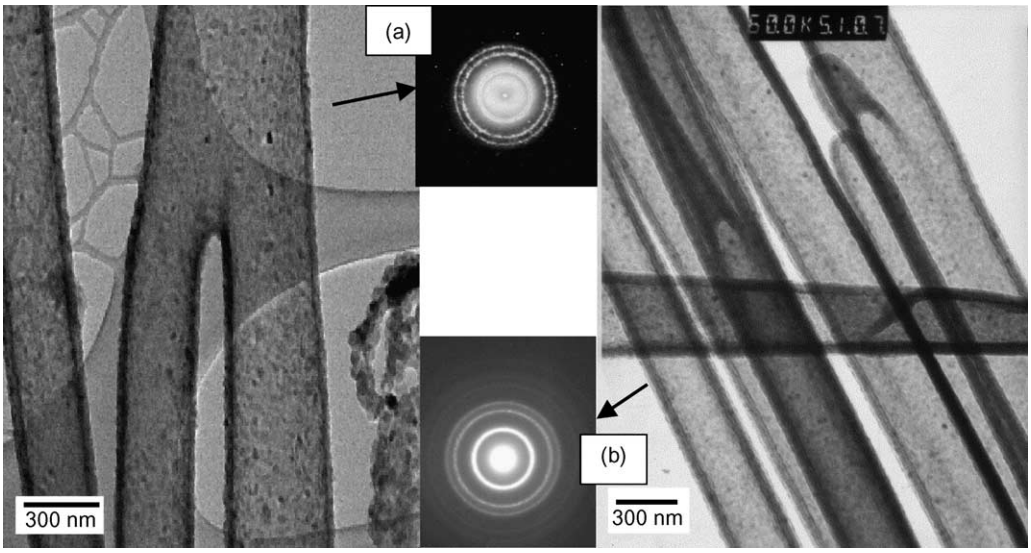

Fig. 4. TEM images and SAED pattern obtained after annealing the CVD-derived SiC nanotubule samples in Ar at 1600 °C.

to the variability in SiC_x nanotubule composition and post-annealing microstructure that we have observed. In a hot wall, atmospheric pressure reactor system with a flowing carrier gas and a multi-component carbosilane precursor, such as was employed here, the composition of the precursor vapor stream can vary considerably at different points in the reactor hot zone, effectively concentrating the small amount of C-containing hydrocarbon byproducts, relative to Si-containing species, as the vapor stream proceeds through the reactor. Also the temperature profile of the substrate can play an important role in determining the composition of the deposition product.

In addition to the partially crystallized, intact, nanotubes, some broken SiC nanotubes and small fragments were also observed after the heat treatment. After crystallization, the highly crystalline nanotubes, in particular, appeared to suffer a considerable loss in strength and were easily fragmented on handling or on ultrasonication. The XRD data obtained for the bulk sample after heat-treatment at 1600 °C (4 h) also shows that crystallization of the SiC has occurred. The X-ray diffraction pattern of the heat-treated SiC samples is consistent with that of β-SiC; no other crystalline impurities were observed. The Raman spectrum of these heat-treated SiC nanotubes was taken upon excitation with the 514.5 nm line of an argon ion laser. The absorption peaks observed at 792 and 970 cm^{-1} are consistent with expectations for crystalline β-SiC.[48]

On a few occasions, a small amount of straight nanorods with diameters from 20–100 nm and lengths extending up to several micrometers were also observed, along with the SiC nanotubes, after heat treatment of the as-prepared SiC nanotubes at 1600 °C. HRTEM and SAED revealed that these nanorods were β-SiC single crystals (see below).

3.3. Preparation of SiC nanostructures by polymer pyrolysis

After removal from the alumina templates, the SEM micrographs of the as-prepared SiC nanomaterials obtained from direct heating of alumina membranes infused with the oligomeric/polymeric carbosilanes and PSE were quite similar in external appearance to those observed for the CVD-prepared "SiC" nanotubes. Thus bundles of fibers having a uniform outer surface of 250–300 nm diameter and lengths of ca. 60 μm corresponding to the thickness of the template were observed. Again, a thin layer of SiC that is formed on one end of the fibers serves to hold them in a parallel arrangement after removal of the alumina template, giving a highly aligned, brush-like, configuration for the fiber bundles. Ultrasonication in alcohol at room temperature for a short while (20 s) is sufficient to break up the SiC thin layer and separate the individual fibers, although the yield of intact 60 μm fibers was somewhat less in this case, due apparently to the relatively weaker nature of these fibers. Details of the morphology of one of these types of SiC nanofibers are shown in the TEM images in Fig. 5.

The halo-like ring patterns in the corresponding selected area electron diffraction (SAED) (inset) revealed that these SiC nanofibers were completely amorphous. However, in these cases the nanofibers are neither completely solid nanorods nor hollow nanotubes, but instead have porous fiber or bamboo-like structures with wall thicknesses of 20–50 nm in the hollow portion of the bamboo-like fibers. The average composition of individual bundles (5) of the bamboo-like nanofibers obtained from the carbosilane mixture were determined by EMPA (43.7 wt.% Si; 25.0 wt.% C; and 19.4 wt.% O), revealing a substantial amount of oxygen, in addition to C and Si, in this case ($Si_1C_{1.3}O_{0.8}$). The high oxygen content in

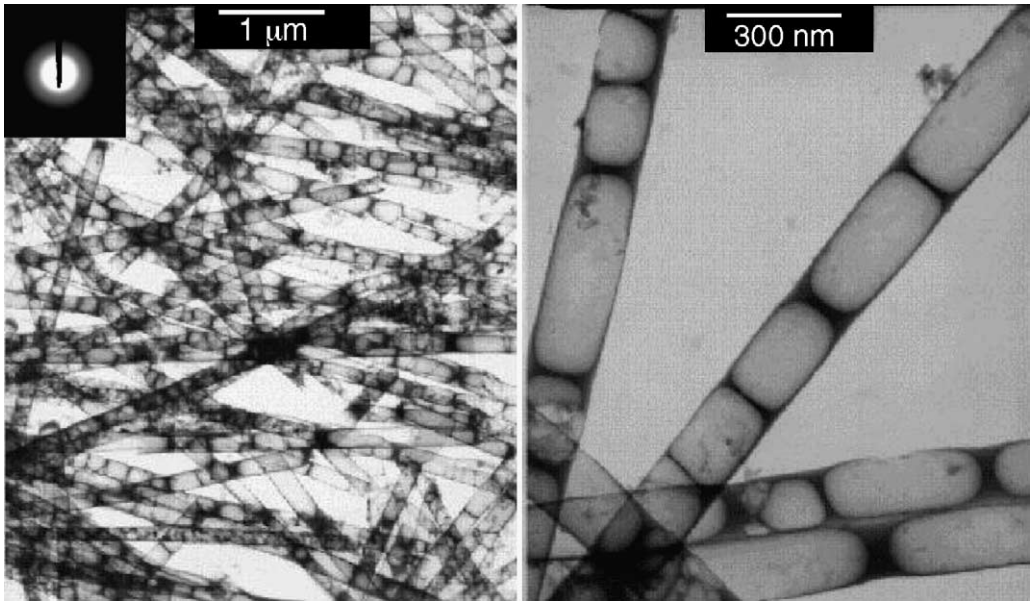

Fig. 5. TEM images and SAED pattern obtained for the bamboo-like nanofibers derived by polymer pyrolysis.

this case may be due to the reaction of the Si–H containing polymers employed with adventitious oxygen or adsorbed water during the infusion of these polymers into the alumina membranes, or upon heating to pyrolyze the polymers, as neither of these polymers contained substantial oxygen initially.

The use of pentane solutions of the precursors instead of the neat carbosilanes seemed to produce a higher proportion of the bamboo-like fibers but, in our hands, did not lead to completely hollow SiC nanotubes. The formation of tubules versus solid (or porous) fibers upon pyrolysis of such precursor polymers in nanoporous alumina templates clearly depends on a variety of factors, including the amount of precursor present in the nanopores, its tendency to adsorb onto the alumina wall surface versus self-associate as droplets throughout the nanopore, the changes in volume, composition and adherence occurring during pyrolysis of the precursor, including the need to eliminate the gases, as well as the structure of the final solid product (layered versus a 3D network structure).

These amorphous nanofibers can be crystallized by heat treatment at 1600–1650 °C in argon. However, the annealing changed significantly the morphologies of these as-prepared nanofibers. Fig. 6 shows some typical TEM images and a SAED pattern for the product obtained after annealing a sample of nanobamboo-like fibers at 1600 °C for 4 h. The aligned and brush-like nanofiber bundles had disappeared, leaving a collection of randomly distributed, dense, nanorods, plus some crystalline SiC nanoparticles (average diameter ca. 40 nm) and a few sections of the larger diameter, unconverted, SiC nanofibers.

The nanorods had high aspect ratios (length/diameter) of up to ca. 100:1 with lengths up to several micrometers and diameters of 50–200 nm. HRTEM showed these to be essentially single crystal SiC nanorods, much like those observed as a very minor product in the CVD-derived samples (see above), but in much higher proportion (as much as 40–50%) relative to the other products in this case. When the time in the annealing furnace at 1600 °C was reduced from 4 to 1 h, the sample was found to contain relatively few crystalline SiC nanorods; however, extensive breakdown of the initial nanofibers into a fine-grained powder was observed, suggesting that the nanorods are formed from the powder rather than directly from (or in) the nanofibers.

In these annealing studies, in order to avoid the oxidation of SiC at high temperature by residual O_2 in the argon carrier gas, a carbon cloth was used to cover the Mo boats that contained the nanofiber samples. As a comparison, annealing without the carbon cloth was also examined. Under the same annealing conditions, the products obtained without the carbon cloth contained far fewer SiC nanorods (only about 5%). Therefore, it is clear that the presence of the C cloth, as well as the initial composition of the amorphous ceramic starting material, plays an important part in the formation of these SiC nanorods.

Three different mechanisms have been identified in past work involving the growth of SiC nanorods.[29–36] One is the vapor–liquid–solid (VLS) growth mechanism (usually involving a liquid metal catalyst); the other two are the conventional spiral growth mechanism and the VS growth process. There were no droplets observed at the end of any of the nanorods, which are the most characteristic sign of the VLS mechanism. Similarly, the lack of spiral nanowires in these TEM images appears to rule out the spiral growth mechanism. Thus, the growth of the SiC nanorods in this case appears to be more consistent with expectations for a VS growth mechanism.

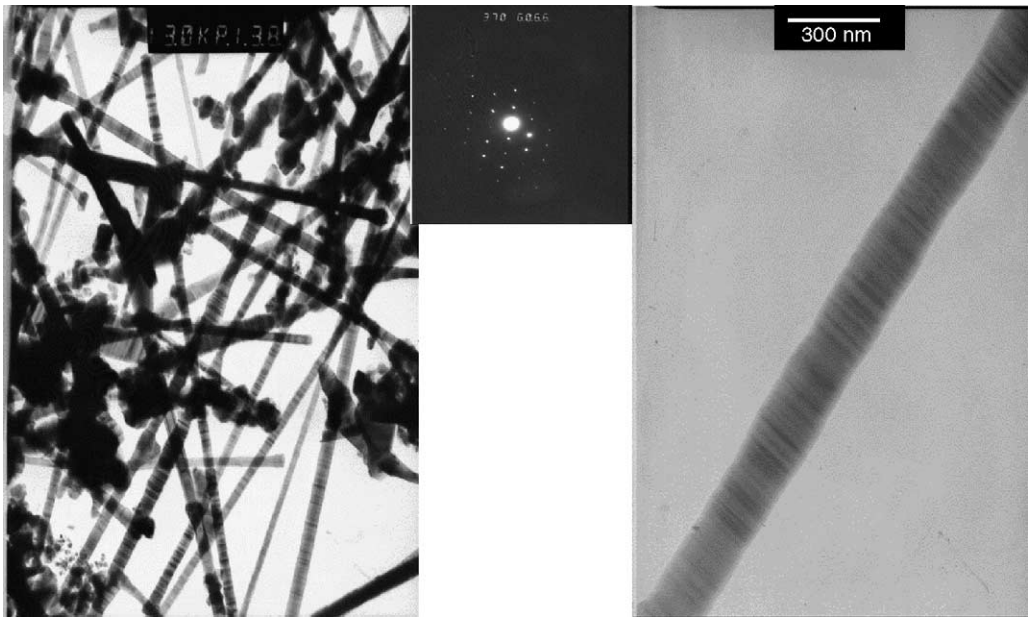

Fig. 6. TEM images and SAED patterns for the single-crystal β-SiC nanorods obtained upon annealing the bamboo-like nanofibers derived by polymer pyrolysis.

It is perhaps notable that, in the case of the carbosilane-derived nanofibers, the starting material for the annealing experiments contains a significant amount of oxygen, as well as silicon and carbon ($Si_1C_{1.3}O_{0.8}$), and is thus is best described as a silicon oxycarbide, rather than as amorphous SiC_x. Moreover, our observations suggested that the initially obtained SiC_xO_y nanofibers were not stable at 1600 °C and that they underwent fragmentation to form small particles, before forming crystalline SiC nanorods. At these temperatures, the rapid decomposition of silicon oxycarbide is known to occur, leading to $SiO_{(g)}$ and $CO_{(g)}$, and ultimately, disproportionation to crystalline SiO_2 and SiC.[49] This would explain the breakdown of the initial nanofiber structure into smaller particles, as the crystallization and the loss of gaseous species proceeds. The $SiO_{(g)}$ and $CO_{(g)}$ could then react directly at some nucleation site (presumably the surface of a β-SiC crystallite) to grow β-SiC nanorods via the VS mechanism. The reaction, $SiO_{(g)} + 2CO_{(g)} \rightarrow SiC_{(s)} + CO_{2(g)}$, which has been suggested in at least one other case of SiC whisker growth from intimate mixtures of sol–gel derived SiO_2 and C[30] may also to be operative here. In addition to the decomposition reaction, the CO in this reaction could also be coming from the reaction of residual oxygen in the Ar gas stream with the carbon cloth covering the sample container, which is supported by the observation that the use of a C cloth over the sample container leads to a higher proportion of β-SiC nanorods in the final reaction product.

Acknowledgements

We are grateful to the NASA Glenn Research Center's Ultra Efficient Engine Technology Program for their financial support of this work. We thank Dr. David Wark and Kiera Becker of the R.P.I. Department of Earth and Environmental Sciences for assistance with the electron microprobe analyses and Chris Whitmarsh of Starfire Systems, Inc. for help with the 1600 °C annealing of the samples. We also thank Dr. David Hull of the NASA Glenn Research Center who carried out some of the HRTEM studies that are reported herein and Prof. P. Ajayan of the R.P.I. Materials Department and his students for helpful discussions and advice.

References

1. (a) Larkin, D. and Interrante, L. V., *Chem. Mater.*, 1992, **4**, 22;
   (b) Larkin, D. J. and Interrante, L. V., *Springer Proc. Phys.*, 1992, **71**, 239;
   (c) Lienhard, M. A., Interrante, L. V. and Larkin, D. J., *MRS Symp. Proc.*, 1998, **495**, 139.
2. AHPCS is a partially allyl-substituted polycarbosilane with a hyperbranched structure of the type, $[R_3SiCH_2-]_x[-SiR_2CH_2-]_y[=SiR(CH_2-)]_z[\equiv Si(CH_2-)]_l$, R = H or allyl ($CH_2=CHCH_2-$); sold by Starfire Systems Inc., Saratoga Technology & Energy Park, 10 Hermes Road, Suite 100, Malta, NY 12020; http://www.starfiresystems.com/.
3. Rushkin, I., Shen, Q., Lehman, S. E. and Interrante, L. V., *Macromolecules*, 1997, **30**, 3141.
4. Moraes, K. and Interrante, L. V., *J. Am. Ceram. Soc.*, 2003, **86**, 342.
5. (a) Interrante, L. V., Wu, H.-J., Apple, T., Shen, Q., Ziemann, B., Narsavage, D. M. *et al.*, *J. Am. Chem. Soc.*, 1994, **116**, 12085;
   (b) Shen, Q. and Interrante, L. V., *Macromolecules*, 1996, **29**, 5788.
6. Lienhard, M., Rushkin, I., Apple, T., Verdecia, G. and Interrante, L. V., *J. Am. Chem. Soc.*, 1997, **119**, 12020.
7. Liu, Q., Wu, H.-J., Lewis, R., Maciel, G. E. and Interrante, L. V., *Chem. Mater.*, 1999, **11**, 2038.
8. (a) Whitmarsh, C. and Interrante, L. V., *Organometallics*, 1991, **10**, 1336;
   (b) Whitmarsh, C. W. and Interrante, L. V., US Patent 5,153,295.
9. Ning Lu, Leonard, V. and Interrante, *Polym. Mater. Sci. Eng.*, 2003, **89**, 418.
10. Soraru, G. D., Liu, Q., Interrante, L. V. and Apple, T., *Chem. Mater.*, 1998, **10**, 4047.
11. Zheng, C.-F. and Interrante, L. V., in press.
12. Shen, Q., Ph.D. thesis. Rensselaer Polytechnic Institute, 1995.
13. (a) Interrante, L. V., Jacobs, J. M., Sherwood, W. and Whitmarsh, C. W., *Key Eng. Mater.*, 1997, **127–131**, 271;
   (b) Interrante, L. V., Moraes, K., MacDonald, L. and Sherwood, W., *Ceram. Trans.*, 2002, **144**, 125.
14. (a) Sherwood, W. J., CMCs come down to earth. *Am. Ceram. Soc. Bull.*, 2003, **82**(8), 25;
   (b) Hayes, S., Sherwood, W. J., Stiles, D., Voorhees, C., Porter, W., Riester, L., *et al.*, In *Edgar. Ceram. Eng. Sci. Proc., Vol 24 (4, 27th International Cocoa Beach Conference on Advanced Ceramics and Composites, 2003: Part B)*, 2003, p. 555.
15. Moraes, K., Vosburg, J., Wark, D., Interrante, L. V., Puerta, A. R., Sneddon, L. G. *et al.*, *Chem. Mater.*, 2004, **16**, 125.
16. Huczko, A., *Appl. Phys. A*, 2000, **70**, 365.
17. Pender, M. J. and Sneddon, L. G., *Chem. Mater.*, 2000, **12**, 280.
18. Che, G., Lakshimi, B. B., Martin, C. R., Fisher, E. R. and Ruoff, R. R., *Chem. Mater.*, 1998, **10**, 260.
19. (a) Hulteen, J. C. and Martin, C. R., *J. Mater. Chem.*, 1997, **7**, 1075;
   (b) Martin, C. R., *Chem. Mater.*, 1996, **8**, 1739.
20. Lakshimi, B. B., Patrissi, C. J. and Martin, C. R., *Chem. Mater.*, 1997, **9**, 2544.
21. Iijima, S., *Nature (London)*, 1991, **354**, 56.
22. Chopra, N. G., Luyken, R. J., Cherrey, K., Crespi, V. H., Cohen, M. L., Louie, S. G. *et al.*, *Science*, 1995, **269**, 966.
23. Weng-Sieh, Z., Cherrey, K., Chopra, N. G., Blase, X., Miyamoto, Y., Rubio, A. *et al.*, *Phys. Rev. B*, 1995, **51**, 11229.
24. (a) Feldman, Y., Wasserman, E., Srolovitt, D. J. and Tenne, R., *Science*, 1995, **267**, 222;
   (b) Tenne, R., Margulis, L., Genut, M. and Hodes, G., *Nature (London)*, 1992, **360**, 444.
25. Satishkumar, B. C., Govindaraj, A., Vogl, E. M., Basumallick, L. and Rao, C. N. R., *J. Mater. Res.*, 1997, **12**, 604.
26. (a) Dloczik, L., Engelhardt, R., Ernst, K., Fiechter, S., Sieber, I. and Koenenkamp, R., *Appl. Phys. Lett.*, 2001, **78**, 3687;
   (b) Hacohen, Y. R., Grunbaum, E., Tenne, R., Sloan, J. and Hutchison, J. L., *Nature (London)*, 1998, **395**, 336;
   (c) Li, J. Y., Chen, X. L., Qiao, Z. Y., Cao, Y. G. and Li, H., *J. Mater. Sci. Lett.*, 2001, **20**, 1987;
   (d) Awasthi, K., Singh, A. K. and Srivastava, O. N., *J. Nanosci. Nanotechnol.*, 2002, **2**, 67.
27. Fissel, A., Schroter, B. and Richter, W., *Appl. Phys. Lett.*, 1995, **66**, 3182.
28. Jacques, S., Guette, A., Langlais, F. and Naslain, R., *J. Mater. Sci.*, 1997, **32**, 983.
29. Dai, H. J., Wong, E. W., Liu, Y. Z., Fan, S. S. and Lieber, C. M., *Nature (London)*, 1995, **375**, 769.

30. Han, W. Q., Fan, S. S., Li, Q. Q., Liang, W. J., Gu, B. L. and Yu, D. P., *Chem. Phys. Lett.*, 1997, **265**, 374.
31. Wong, E. W., Sheehan, P. E. and Lieber, C. M., *Science*, 1995, **277**, 1971.
32. Pan, Z. W., Lai, H. L., Au, F. C. K., Duan, X. F., Zhou, W. Y., Shi, W. S. *et al.*, *Adv. Mater.*, 2000, **12**, 1186.
33. (a) Zhou, X. T., Wang, N., Lai, H. L., Peng, H. Y., Bello, I., Wong, N. B. *et al.*, *Appl. Phys. Lett.*, 1999, **74**, 3942;
(b) Wong, K. W., Zhou, X. T., Frederick, C. K., Au, C. K., Lai, H. L., Lee, C. S. *et al.*, *Appl. Phys. Lett.*, 1999, **75**, 2918;
(c) Seeger, T., Redlich, P. and Muehle, M., *Adv. Mater.*, 2000, **12**, 279;
(d) Zhu, Y. Q., Hu, W. B., Hsu, W. K., Terrones, M., Grobert, N., Hare, J. P. *et al.*, *J. Mater. Chem.*, 1999, **9**, 3173.
34. Meng, G. W., Zhang, L. D., Qin, Y., Feng, S. P., Mo, C. M., Li, H. J. *et al.*, *J. Mater. Sci. Lett.*, 1999, **18**, 1255.
35. Zhou, X. T., Wang, N., Au, F. C. K., Lai, H. L., Peng, H. Y., Bello, I. *et al.*, *Mater. Sci. Eng.*, 2000, **A286**, 119.
36. Hu, J.-Q., Lu, Q.-Y., Tang, K.-B., Qian, Y.-T., Zhou, G.-E., Liu, X.-M. *et al.*, *Chem. Mater.*, 1999, **11**, 2369.
37. It should be noted that SiC, which normally forms stable, 3D network, structures that involve sp3 hybridized Si and C, is not likely to form a direct analog to single wall carbon nanotubes (SWCNTs), which requires sp2 hybridization; however, a recent theoretical calculation [Menon, M., Richter, E., Mavrandonakis, A., Froudakis, G. and Andriotis, A. N., *Phys. Rev. B*, 2004, **69**, 115322] has suggested that a somewhat distorted (and undoubtedly highly reactive) version of a SWCNT might be possible.
38. (a) Keller, N., Pham-Huu, C., Ledoux, M. J., Estournes, C. and Ehret, G., *Appl. Catal. A.*, 1999, **187**(2), 255;
(b) Keller, N., Pham-Huu, C., Ehret, G., Keller, V. and Ledoux, M. J., *Carbon*, 2003, **41**, 2131.
39. Nhut, J.-M., Viera, R., Pesant, L., Tessonnier, J.-P., Keller, N., Ehret, G. *et al.*, *Catal. Today*, 2002, **76**, 11.
40. Sun, X.-H., Li, C.-P., Wong, W.-K., Lee, C.-S., Lee, S.-T. and Teo, B.-K., *J. Am. Chem. Soc.*, 2002, **124**, 14464.
41. Forsthoefel, K. M., Pender, M. J. and Sneddon, L. G., *MRS Symp. Proc.*, 2002, **53**, 59.
42. Martin, C. R., *Science*, 1994, **266**, 1961.
43. Schmid, G., *J. Mater. Chem.*, 2002, **12**, 1231.
44. Goldstein, J. I., Newbury, D. E., Echlin, P., Joy, D. C., Fiori, C. and Lifshin, E., *Scanning Electron Microscopy and X-Ray Microanalysis*. Plenum Press, New York, 1981, p. 673.
45. Lienhard, M., to be reported elsewhere.
46. Puddemann, E. P., *Saline Coupling Agents* (*2nd ed.*). Plenum, New York, 1991.
47. Kohli, P. and Martin, C. R., *Drug News Perspect.*, 2003, **16**(9), 566–573.
48. Shi, W. S., Zheng, Y. F., Peng, H. Y., Wang, N., Lee, C. S. and Lee, S. T., *J. Am. Ceram. Soc.*, 2000, **83**, 3228.
49. Soraru, G. D. and Suttor, D., *J. Sol–Gel Sci. Technol.*, 1999, **14**(1), 69–74.